

# Self-Pivoting Convex Quadrangles

Paris Pamfilos

**Abstract.** In this article we examine conditions for the existence of pivoting circumscriptions of a convex quadrangle  $q_1$  by another quadrangle  $q$  similar to  $q_1$ , pivoting about a fixed point. There are 8 types of such circumscriptions and we formulate the restrictions on the quadrangles of each type, imposed by the requirement of such a circumscription. In most cases these restrictions imply that the quadrangles are cyclic of a particular type, in one case are harmonic quadrilaterals, and in two cases are trapezia of a special kind.

## 1. Possible configurations

Given two convex quadrangles  $\{q_1 = A_1B_1C_1D_1, q_2 = A_2B_2C_2D_2\}$ , we study the circumscription of a quadrangle  $q = ABCD$ , which is similar to  $q_2$ , about the quadrangle  $q_1$ . Disregarding, for the moment, the right proportions of sides, and focusing only on angles, we can easily circumscribe to  $q_1$  quadrangles  $q$  with the same *angles* as those of  $q_2$  and in the same succession. For this, it suffices to consider the circles  $\{\kappa_i, i = 1, 2, 3, 4\}$ , the points of each viewing corresponding

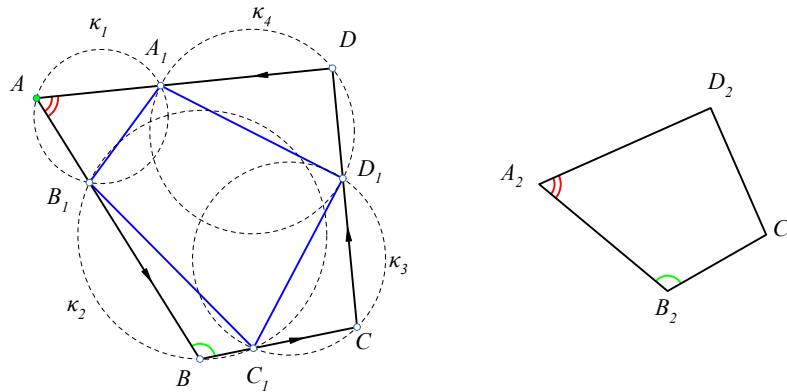


Figure 1. Circumscribing  $q_2$  about  $q_1$

sides of  $q_1$  under corresponding angles of  $q_2$  or their supplement. Then, taking an arbitrary point  $A$  on  $\kappa_1$ , we draw the line  $AB_1$  intersecting  $\kappa_2$  at  $B$ , then draw the line  $BC_1$  intersecting  $\kappa_3$  at  $C$  and so on (See Figure 1). It is trivial to see that the procedure closes and defines a circumscribed quadrangle with the same angles as  $q_2$ . Below we refer to this construction as “*the standard circumscription procedure*” (SCP). By this, the resulting quadrangles  $q$  have the same angles as  $q_2$

but in general not the right proportions of sides, that would make them similar to  $q_2$ .

There are here several possible configurations, that must be considered, since a vertex of  $q$ ,  $A$  say, can be opposite or “view” any of the four sides of  $q_1$ . Each vertex of  $q_2$  and each side of  $q_1$  give, in principle, two possibilities for circumscription, corresponding to equally or oppositely oriented quadrangles. Fixing the side  $A_1B_1$  and considering all possibilities for the opposite to it angle of  $q$  together with the possible orientations, we see that there are in total 8 possibilities. We call each of them a “circumscription type of  $q_2$  about  $q_1$ ” and denote it by  $q_2(q_1, X)^\pm$ . In this notation  $X$  stands for the vertex of  $q_2$  opposite to the side  $A_1B_1$  of  $q_1$  and the sign denotes the equal or inverse orientation of the circumscribing to the circumscribed quadrangle. Thus, in figure-1 the symbol denoting the case would be  $q_2(q_1, A)^+$ .

In general there are 8 different types of circumscription, each type delivering infinite many circumscribed quadrangles  $q$  with the same angles as  $q_2$ . In some special cases the number of types can be smaller, as f.e. in the case of a circumscribing square, in which there is only one type. We stress again the fact, that if we stick to a type and repeat the procedure SCP, starting from arbitrary points  $A \in \kappa_1$ , we obtain in general quadrangles with the same angles as  $q_2$  but varying ratios of side-lengths. There is an exceptional case in this procedure, which produces circumscribed quadrangles  $q$  of the same similarity type, for every starting position of  $A$  on  $\kappa_1$ . This is the “pivotal case” examined in the next section.

### 2. The pivotal case

This type of circumscription, besides the quadrangle  $q_1 = A_1B_1C_1D_1$ , which we circumscribe, it is characterized by an additional point, the “pivot”, not lying on the side-lines of  $q_1$ . The pivot, for a generic convex quadrangle, defines four circles  $\kappa_1 = (A_1B_1P)$ ,  $\kappa_2 = (B_1C_1P)$ ,  $\kappa_3 = (C_1D_1P)$ , and  $\kappa_4 = (D_1A_1P)$  (See

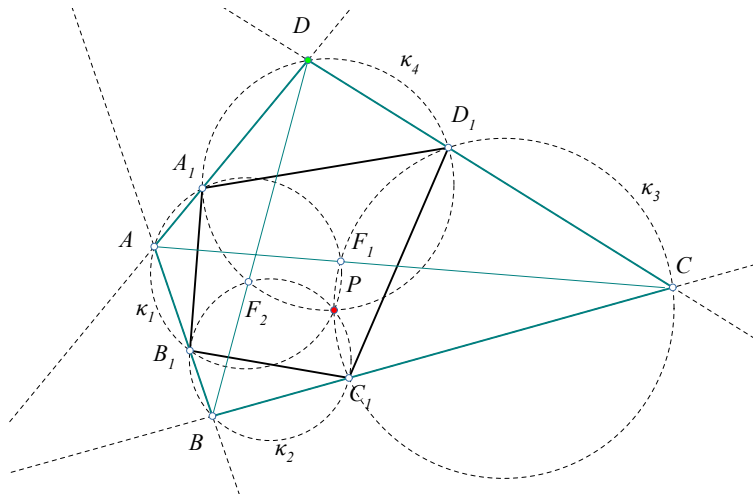


Figure 2. The pivotal case

Figure 2), and through them a circumscribed quadrangle  $q = ABCD$ , that can be non convex, even degenerate in the case  $P$  is the *Miquel Point* of the complete quadrilateral generated by  $q_1$  ([8, p.139]). Having the circles  $\{\kappa_i\}$ , a circumscribed quadrilateral can be defined by starting from an arbitrary point  $A$  on  $\kappa_1$  and applying the SCP procedure. Measuring the angles at the second intersection point  $F_1$  of the circles  $\{\kappa_1, \kappa_3\}$

$$\widehat{AF_1P} = \widehat{PB_1B} \quad \text{and} \quad \widehat{CF_1P} = \widehat{PC_1C}$$

we see that  $F_1$  is on the diagonal  $AC$  of  $q$ . Analogously we see that the intersection point  $F_2$  of the other pair of opposite lying circles  $\{\kappa_2, \kappa_4\}$  is on the diagonal  $BD$  of  $q$ . This implies that the triangles created by the diagonals of  $q$  are of fixed similarity type, independent of the position of  $A$  on  $\kappa_1$ . Thus, we obtain an infinity of pairwise similar quadrangles circumscribing  $q_1$  in a way that justifies the naming “pivoting”.

At this point we should notice that the *pivotal* attribute is a characteristic of a particular *type of circumscription of  $q_2$  about  $q_1$* . The same  $q_2$  can have a pivotal type of circumscription about  $q_1$  and at the same time have also another type of circumscription, which is non-pivotal. Figure 3 shows such a case. The quadrangle

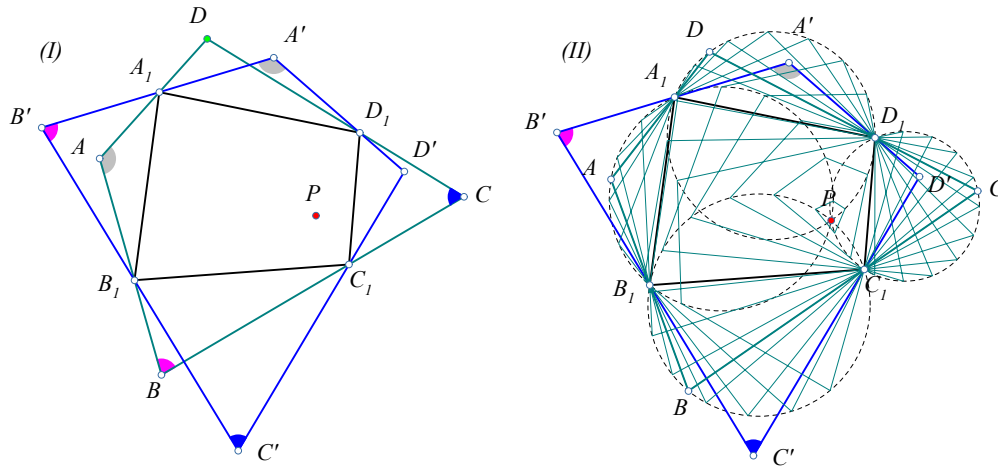


Figure 3. A pivoting circumscription and a non-pivoting one

$q = q_2 = ABCD$  is pivotal about  $q_1$  with shown pivot  $P$ . This circumscription is described by the symbol  $q_2(q_1, A)^+$ . The other quadrangle  $q' = A'B'C'D'$ , circumscribing  $q_1$ , is similar to  $q = q_2$ , but it is not pivotal. Opposite to side  $A_1B_1$  has the angle  $\widehat{B}$  of  $q_2$ , its symbol being  $q_2(q_1, B)^+$ . The characteristic property of the pivotal circumscription is formulated in the next theorem.

**Theorem 1.** *The convex quadrangle  $q_2$  is pivotal of a given type for  $q_1$ , if and only if the pedal quadrangle of  $q_2$  w.r. to some point  $P$  is similar to  $q_1$  and  $q_2$  has the given type w.r to that pedal.*

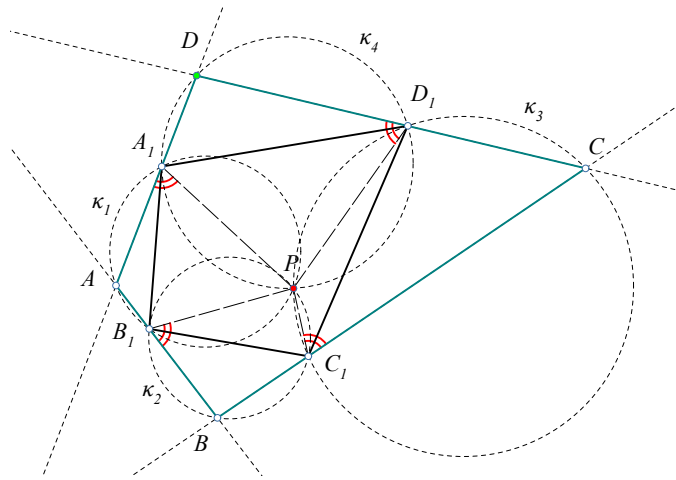


Figure 4. Pivotal  $q$  about its pedal (similar to)  $q_1$

*Proof.* The proof follows from the equalities of the angles shown in figure 4, which results easily from the inscribed quadrangles in the circles  $\{\kappa_i\}$ . These angles vary with the location of the point  $A$  on  $\kappa_1$  and become right when  $A$  obtains the diametral position of  $P$  on  $\kappa_1$ , showing that  $q_1$  is then the pedal of  $q_2 = ABCD$  w.r. to  $P$ . The inverse is equally trivial. If  $q_1$  is the pedal of  $P$ , then, per definition, the segments  $\{PA_1, PB_1, \dots\}$  are orthogonal to the sides  $\{DA, AB, \dots\}$  and the circles  $\{\kappa_i\}$  are defined and carry the vertices of quadrangles  $ABCD$ , pairwise similar and pivoting about  $P$ .  $\square$

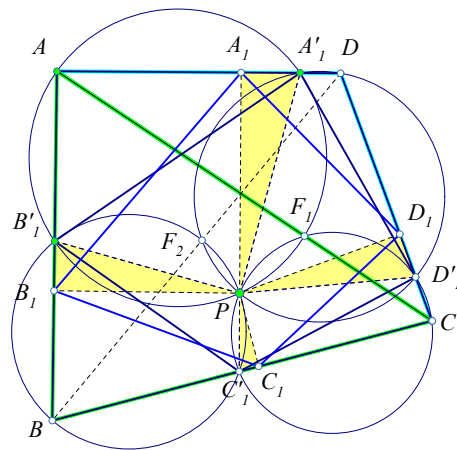


Figure 5. Pedal and dual viewpoint

There is an interesting dual view of the pivotal circumscription, which we should notice here (See Figure 5), but which we do not follow further in the sequel. If

$q_1 = A_1B_1C_1D_1$  is the pedal of  $q = ABCD$  w.r. to some point  $P$ , then turning the projecting lines  $\{PA_1, PB_1, \dots\}$  by the same angle  $\phi$ , we obtain points  $\{A'_1, B'_1, \dots\}$  on the sides of  $q$ , defining the quadrangle  $q'_1 = A'_1B'_1C'_1D'_1$ , similar to  $q_1$  and inscribed in  $q$ . Taking the obvious similarity  $f$  to draw  $q'_1$  back to  $q_1$  and applying it to  $q$ , we find  $q' = f(q)$  similar to  $q$  and circumscribing  $q_1$ . Thus, pivotal circumscriptions about a point are dual and correspond, in this sense, to some pivotal inscriptions about the same point and with the same similarity types of the involved quadrangles.

### 3. Self-pivoting quadrangles

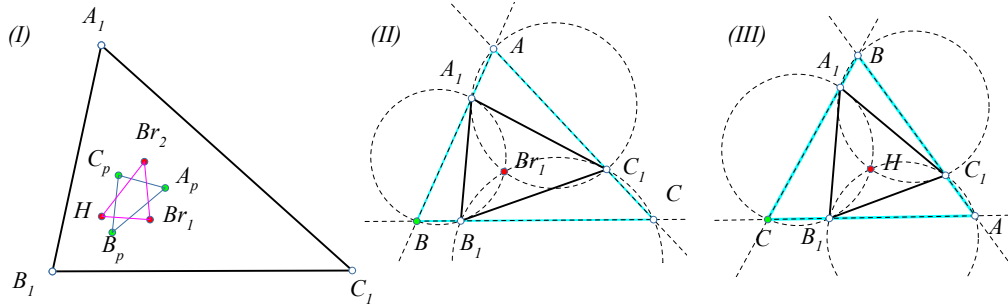


Figure 6. Triangle self-pivoting about a Brocard point and the orthocenter

By “self-pivoting” is meant a convex quadrangle  $q$  that allows pivotal circumscriptions by quadrangles  $q'$  similar to  $q$ . The corresponding problem for triangles leads to the two well known Brocard points  $\{Br_1, Br_2\}$  ([7, p.94], [9, p.117]), the orthocenter  $H$  and three additional points  $\{A_p, B_p, C_p\}$  (See Figure 6-I), which, for a generic triangle, are the 6 internal pivots of circumscribed triangles  $ABC$  similar to the triangle of reference  $A_1B_1C_1$ . Thus, every triangle is self-pivoting in all possible ways, which means that the pivoting triangle  $ABC$  may have opposite to  $A_1B_1$  any of the three angles of the triangle and the orientation of the circumscribing can be the same or the opposite of the circumscribed one.

The situation for quadrangles is quite different. A quadrangle may not allow a pivotal circumscription by quadrangles similar to itself or allow the pivotal circumscription for some types of circumscription only. In the sections to follow we investigate the possibility of self pivotal circumscription by one of the 8 types of circumscription, which, in principle, could be possible and are schematically displayed in figure 7. The symbols used are abbreviations of those introduced in the preceding section,  $q$  denoting the similarity type of a convex quadrangle. Thus, the symbol  $q(A)^+$  denotes a pivoting configuration, in which the circumscribed and the circumscribing quadrangle have the same orientation, are both of the similarity type of the quadrangle  $q = ABCD$ , and the circumscribing has its vertex  $A$  lying opposite to the side  $AB$  of the circumscribed quadrangle.

Looking a bit closer to the different types, reveals some similarities between them, implying similarities of the corresponding circumscription structures. For

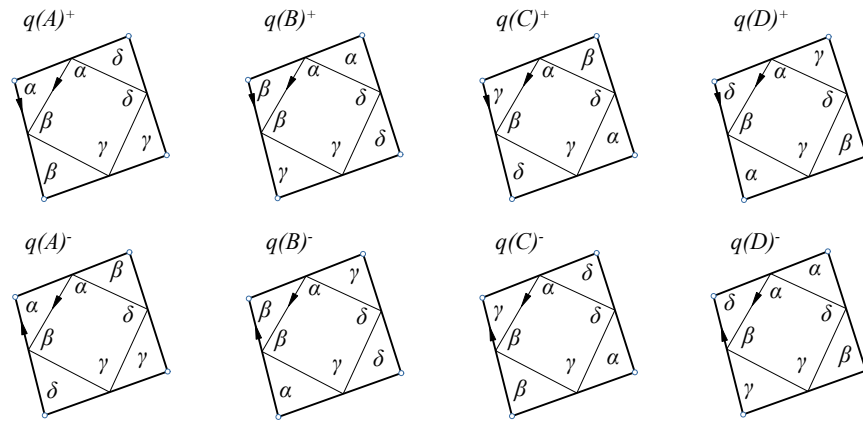


Figure 7. Types of self-pivoting quadrangles  $q' \sim q$  about  $q$

instance, the first two types  $\{q(A)^+, q(B)^+\}$  are the only types for which each vertex  $X$  of the circumscribing is viewing a side  $VW$  of the circumscribed by an angle  $\phi$ , which is also adjacent to the side  $VW$  of the circumscribed quadrangle. We could call this phenomenon an “*adjacent angle side viewing*” of the vertex  $X$  and use for it the acronym ASV. Thus, for these two types all four vertices have the ASV property. The next two  $\{q(C)^+, q(D)^+\}$  are the only circumscription types which have no vertices with the ASV property. Finally, for all other types the ASV property is valid for precisely two vertices lying oppositely. The following discussion shows that self-pivoting quadrangles with the same number of ASV vertices have some common geometric properties, e.g. the types  $\{q(C)^+, q(D)^+\}$  consist of trapezia of a particular kind (section 7).

#### 4. The types $q(A)^+$ and $q(B)^+$

The symbol  $q(A)^+$  resp.  $q(B)^+$ , represents the pivotal circumscription of a quadrangle by one similar to itself and equally oriented, opposite to side  $AB$  having the angle  $\widehat{A}$  resp.  $\widehat{B}$ . Figure 8 shows an example of the type  $q(B)^+$ . The characteristic of  $q(B)^+$  is that the circle  $\kappa_1$  carrying the vertices  $B$  is tangent to  $B_1C_1$ , the circle  $\kappa_2$  carrying the vertices  $C$  is tangent to  $C_1D_1$  and so on. The type  $q(A)^+$  would change the meaning and orientation of these circles, i.e.  $\kappa'_1$  would carry the vertices of angles  $\widehat{A}$  and would be tangent to  $A_1D_1$ ,  $\kappa'_2$  would carry the vertices of angles  $\widehat{B}$  and would be tangent to  $A_1B_1$  and so on. For these two types, the circumscribing quadrangle  $q$  can take the position and become identical with the circumscribed  $q_1$ . In the case  $q(B)^+$ , shown in the figure, the tangency of the circles to corresponding line-sides of the quadrangle implies that the angles  $\{\widehat{BA_1B_1}, \widehat{CB_1C_1}, \dots\}$  are equal. For the same reason also the lines from the pivot  $P$  to the vertices, make with the sides equal angles

$$\widehat{PA_1B_1} = \widehat{PB_1C_1} = \widehat{PC_1D_1} = \widehat{PD_1A_1} = \omega.$$

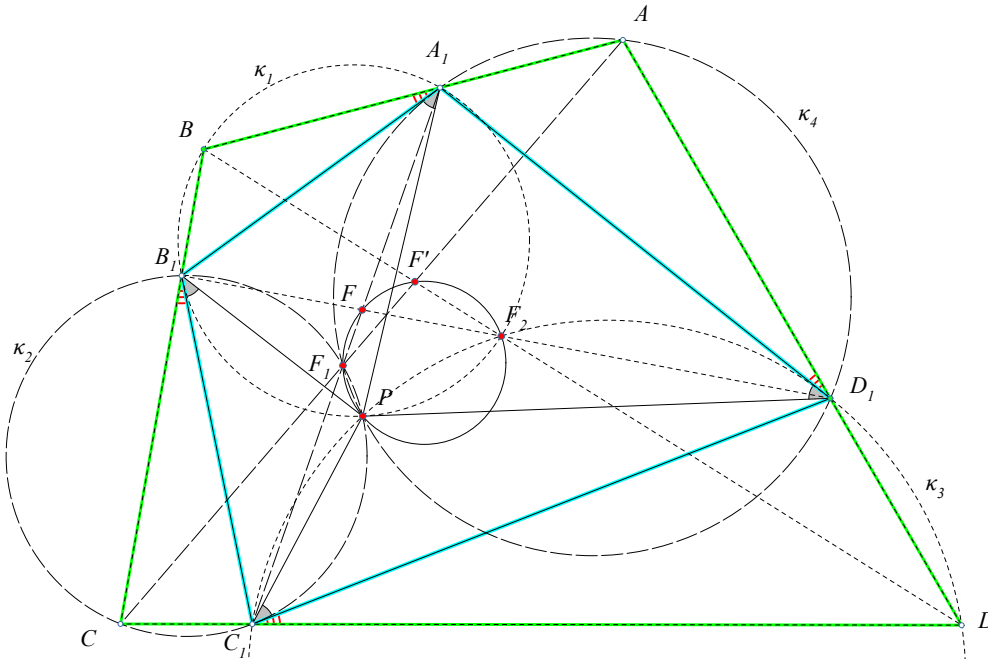


Figure 8. Self-pivoting of type  $q(B)^+$

This is reminiscent of the way the Brocard points of a triangle are defined. In fact, if the quadrangle  $ABCD$  is *cyclic*, then the property of self-pivoting of type  $q(A)^+$  or  $q(B)^+$  is known to be equivalent with the harmonicity of the quadrangle ([6]). In this case the two types occur simultaneously, i.e. if the quadrangle is harmonic, then it is also simultaneously pivotal of type  $q(A)^+$  and  $q(B)^+$ . And if it is cyclic and pivotal of one of these two types, then it is pivotal of the other type too. The corresponding pivots are then the two, so called, “*Brocard points*” of the harmonic quadrangle ([13]) and the angles  $\omega$  for the two pivotal circumscriptions coincide with the, so called, “*Brocard angle*” of the harmonic quadrangle. Next theorem gives a related characterization of the harmonic quadrangle, without to assume that it is cyclic, but deducing this property from the possibility to have simultaneously the two types of pivoting.

**Theorem 2.** *A convex quadrangle  $q_1 = A_1B_1C_1D_1$  is harmonic, if and only if it is simultaneously self-pivoting of type  $q(A)^+$  and  $q(B)^+$ .*

*Proof.* By the preceding remarks, it suffices to show that, if the quadrangle is simultaneously self-pivoting of type  $q(A)^+$  and  $q(B)^+$ , then it is cyclic. For this we use the remark also made in section 2, that the diagonal  $AC$  of a pivoting quadrangle passes through a fixed point  $F_1$  lying on the diagonal  $A_1C_1$  of the circumscribed quadrangle  $q_1$ . This is seen in figure 9-I for the pivoting of type  $q(A)^+$ . The crucial step in the proof is to show that the pivoting of type  $q(B)^+$  has the corresponding  $F'_1$  on  $A_1C_1$  identical with  $F_1$ . This is seen by considering a particular position of the  $q(A)^+$  pivoting, seen in figure 9-II. For this position the diagonal

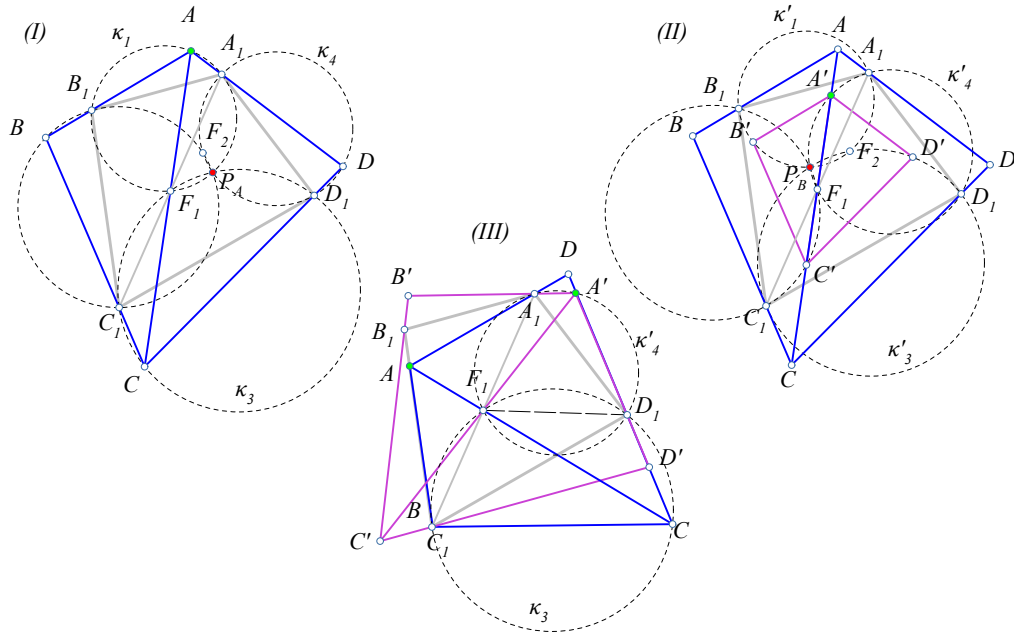


Figure 9. Simultaneous self-pivoting of types  $q(A)^+$  and  $q(B)^+$

$AC$  of the pivoting intersects the circle  $\kappa'_4$  of the  $q(B)^+$  pivoting at a point  $A'$ . This point, taken as vertex of the  $q(B)^+$  pivoting quadrangle  $q' = A'B'C'D'$ , shows that the diagonals  $\{A'C', AC\}$  of the quadrangles  $q'$  and  $q = ABCD$  coincide. Thus, both diagonals pass through the same fixed point of  $A_1C_1$ , thereby proving the coincidence  $F'_1 = F_1$ .

The last step, in proving that  $q$  is cyclic, follows by considering also special positions for the pivoting quadrangles of the two types. These positions are seen in figure 9-III. The quadrangle  $q$  is now taken so that its vertex  $B$  coincides with  $C_1$ , the vertex  $A$  obtaining then a position on  $B_1C_1$ . For the pivoting quadrangle  $q'$  we choose then the position for which  $A'$  is the intersection of  $CD$  with the circle  $\kappa'_4$ , carrying the vertices  $A'$  from which  $A_1D_1$  is seen under the angle  $\widehat{A_1}$ . It is easily verified that the points  $\{D, A', D_1, D', C\}$  are then collinear. Besides, the circles  $\{\kappa'_4, \kappa_3\}$  pass both through  $F_1$  and the quadrangles  $\{A'A_1F_1D_1, D_1F_1C_1C\}$  are cyclic. Considering the angles of these quadrangles, we see that  $\{A'B', CB\}$  are parallel

$$\widehat{A'} + \widehat{C} = \widehat{D_1F_1C_1} + \widehat{D_1F_1A_1} = \pi,$$

which is equivalent with  $\widehat{A} + \widehat{C} = \pi$  and proves the theorem. □

In the rest of this section we describe a general procedure, which, starting with an arbitrary triangle, produces, under some restrictions, general self-pivoting quadrangles of types  $q(A)^+$  or/and  $q(B)^+$ , not necessarily cyclic. We call the corresponding angle  $\omega = \widehat{PA_1B_1} = \widehat{PB_1C_1} = \dots$  the “*Brocard Angle*” of the



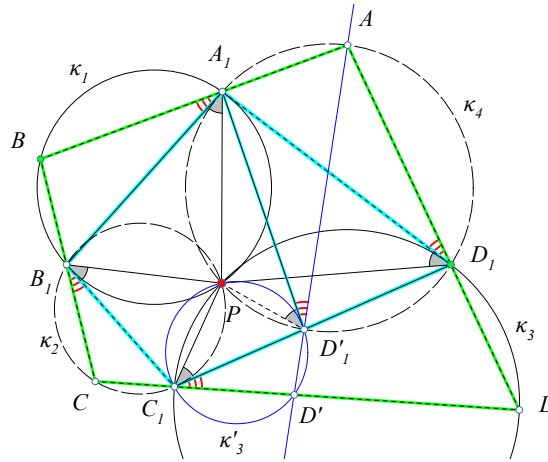


Figure 10. A second self-pivoting of the same type  $q(B)^+$

pivotal circumscription (See Figure 10). First we formulate a simple lemma showing that a self-pivoting quadrangle of this two types is related to other self-pivoting quadrangles of the same type and the same Brocard angle. The lemma, formulated for brevity as a property of the circle  $\kappa_4$  and the type  $q(B)^+$ , holds analogously for the type  $q(A)^+$ , and in both cases the circle  $\kappa_4$  can be replaced, with the necessary adaptation, by any one of the circles  $\{\kappa_i\}$ .

**Lemma 3.** *If the circle  $\kappa_4$ , of a self-pivoting quadrangle  $q_1$  of type  $q(B)^+$ , which is tangent to the side  $A_1B_1$ , has a second intersection  $D'_1$  with the opposite side  $C_1D_1$ , so that  $q'_1 = A_1B_1C_1D'_1$  is convex, then this is also a self-pivoting quadrangle of the same type, with the same angles as  $q_1$ , and the same Brocard angle.*

*Proof.* Referring to the case of figure 10, all that is needed here is to show that the points  $\{D, D'_1, A\}$  are collinear, which follows from a trivial angle chasing argument. The quadrangle  $q'_1 = A_1B_1C_1D'_1$  has the same angles with  $q_1$ , the two angles at  $\{B_1, C_1\}$  being identical and the angles at  $\{A_1, D'_1\}$  being those at  $\{A_1, D_1\}$  permuted.  $\square$

**Corollary 4.** *The two quadrangles  $\{q_1, q'_1\}$  of the preceding lemma, if they exist, they are completely determined by the triangle  $A_1B_1P$  and the position of  $C_1$  on the tangent  $\varepsilon$  of the circumcircle  $\kappa_1$  at  $B_1$ .*

*Proof.* In fact, the given point  $C_1$  determines the circle  $\kappa_2$ . The circle  $\kappa_4$  is determined by its property to be tangent to  $A_1B_1$  at  $A_1$  and the points  $\{D'_1, D_1\}$  are the intersections of circle  $\kappa_4$  with the tangent of  $\kappa_2$  at  $C_1$ . The angle  $\widehat{PA_1B_1}$  of the triangle is the Brocard angle of the circumscription of this type.  $\square$

As is suggested by the lemma and its corollary, not every triangle  $\tau = A_1B_1P$  allows the determination of two points  $\{D_1, D'_1\}$ , defining the two corresponding self-pivoting quadrangles. Depending on the angles of the given triangle  $\tau$  and especially on the angle  $\omega = \widehat{PA_1B_1}$ , destined to play the role of the Brocard

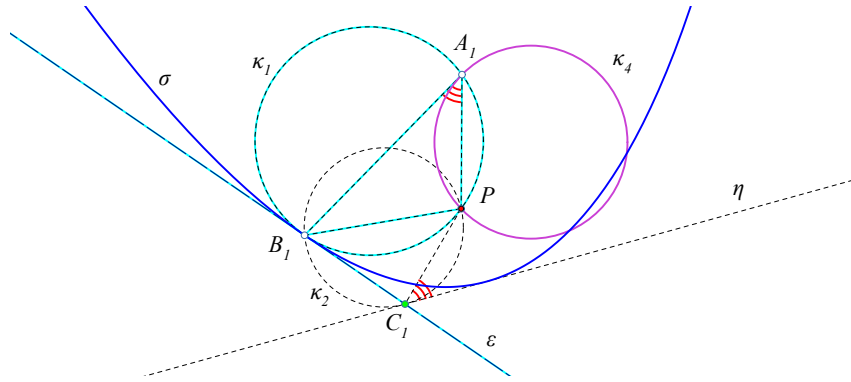


Figure 11. Existence of self-pivoting quadrangles

angle, we may have one, two or none of these points in existence. In fact, consider the points  $C_1$  varying on the tangent  $\varepsilon$  at  $B_1$  to the circumcircle  $\kappa_1$  of  $\tau$  (See Figure 11). Then, by the well known Newton's method to generate conics ([15, p.259], [5, I,p.44]), the lines  $\eta$ , making with  $PC_1$  the constant angle  $\omega$ , envelope a parabola  $\sigma$  with focus at  $P$  and tangent to  $\varepsilon$ . If this parabola has  $\kappa_4$  totally in its inner region, then its tangents cannot have common points with  $\kappa_4$ , i.e. there are no points  $\{D_i\}$ . If  $\sigma$  touches  $\kappa_4$ , then there is only one line  $\eta$  intersecting the circle  $\kappa_4$ , i.e. the points  $\{D_1, D'_1\}$  coincide and we have one solution only. Finally, if

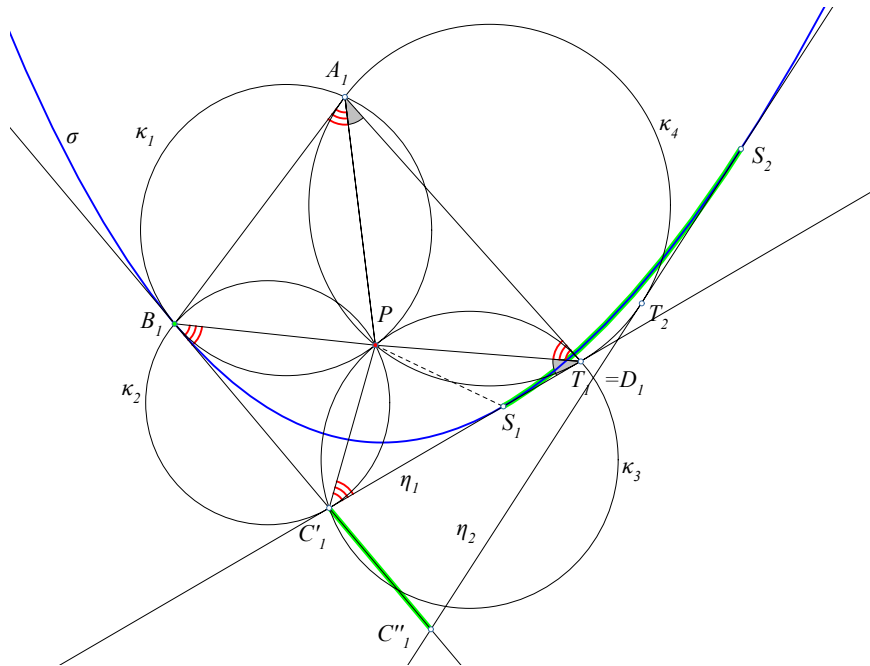


Figure 12. Case in which  $\kappa_4$  intersects the parabola

the circle and the parabola intersect at two points, the common tangents to  $\{\sigma, \kappa_4\}$  define corresponding contact points  $\{T_1, T_2\}$  of the circle, contact points  $\{S_1, S_2\}$  of the parabola and two points  $\{C'_1, C''_1\}$  on  $\varepsilon$  (See Figure 12). The tangents  $\eta = C_1S$  of  $\sigma$  intersect  $\kappa_4$  only if  $C_1$  is in the interval  $C_1 \in [C'_1, C''_1] \subset \varepsilon$ . For the points  $C_1 \in (C'_1, C''_1)$  of the open interval we have two solutions, whereas at the end points  $\{C'_1, C''_1\}$  of this interval we have one solution only. Figure 12 shows the special self-pivoting quadrangle having  $C_1 = C'_1$  and  $D_1$  identical with the corresponding contact point  $T_1$  of the common tangent  $\eta_1$  with  $\kappa_4$ . Notice that the circle  $\kappa_4$  cannot be completely outside of the parabola, since it passes through the focus  $P$  of it. Hence, the cases considered above exhaust the possibilities that may occur, concerning the existence or not of self-pivoting quadrangles of type  $q(B)^+$ , defined from a triangle  $AB_1P$  using this recipe.

**5. The Brocard angle**

In the previous section we defined the Brocard angle of a pivotal circumscription of a quadrangle of the types  $q(A)^+$  and  $q(B)^+$ . This angle is intimately related to the aforementioned generation of parabolas, resulting by varying an angle of fixed measure ([4, p.28]). Figure 13-I shows a consequence of this relation. Here we

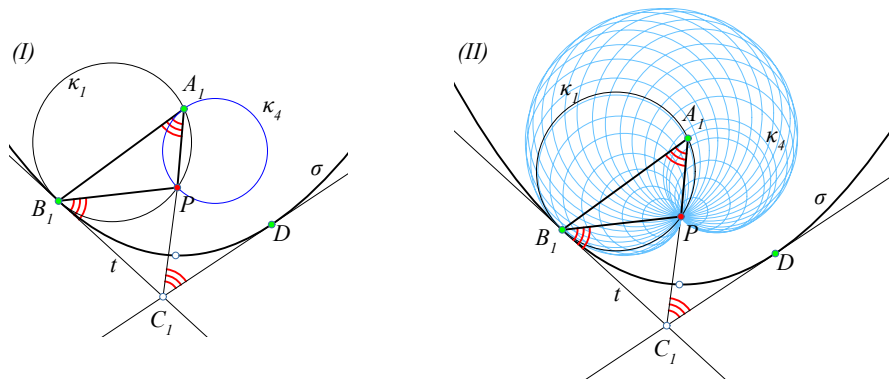


Figure 13. The circles  $\{\kappa_4\}$  for  $A_1 \in \kappa_1$  generate a cardioid

start with a parabola  $\sigma$  and the tangent  $t$  at a point  $B_1$  of it. For every point  $C_1$  on  $t$ , other than  $t$ , tangent to the parabola from  $C_1$  makes with the line  $PC_1$  the same constant angle  $\omega = \widehat{PA_1B_1}$ . The circle  $\kappa_1$  is defined by its property to be tangent to  $\sigma$  at  $B_1$  and pass through the focus  $P$  of the parabola. The points  $A_1$  of  $\kappa_1$  view the segment  $PB_1$  under the fixed angle  $\omega = \widehat{PA_1B_1}$ . If there were a pivotal quadrangle of type  $q(B)^+$  with Brocard angle  $\omega$ , then this would produce such a figure, with the circle  $\kappa_4$  intersecting the parabola. By its definition, the circle  $\kappa_4$  is tangent to  $A_1B_1$  at  $A_1$  and passes through  $P$ . By the discussion in the previous section, in order to have a pivotal circumscription with Brocard angle  $\omega$ , it is necessary and sufficient to have a place of  $A_1$  on  $\kappa_1$ , such that the corresponding circle  $\kappa_4$  intersects the parabola. By varying the position of  $A_1$  on  $\kappa_1$ , we obtain a

one-parameter family of circles  $\kappa_4$ , which will be seen below to envelope a cardioid tangent to  $\sigma$  at  $B_1$  ([1], [11, p.34], [10, p.118], [14, p.73]). Then, the condition of existence of a circle  $\kappa_4$  intersecting the parabola appears to be equivalent with the existence of an intersection point of the cardioid and the parabola, other than  $B_1$ .

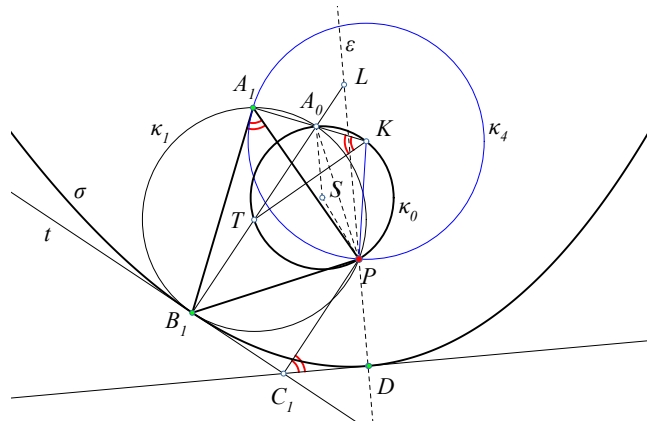


Figure 14. Seeking the position of the cardioid relative to the parabola  $\sigma$

In the sequel we determine the position of the cardioid, relative to the parabola, showing that the value  $\pi/4$  of the Brocard angle  $\omega$  plays an important role, separating the intersecting from the non-intersecting cases. We start with the case  $\omega = \widehat{PA_1B_1} > \pi/4$ , the case  $\omega < \pi/4$  allowing a similar handling. For this, consider the tangent at the vertex  $D$  of the parabola  $\sigma$ , intersecting the tangent  $t$  at the point  $C_1$  (See Figure 14). Let also  $L$  be the intersection point of the axis  $\varepsilon$  of the parabola with the line  $B_1A_0$ , where  $A_0$  is the diametral point of  $B_1$  on  $\kappa_1$ . The quadrangle  $LB_1C_1D$  is cyclic and, since all tangents of  $\sigma$  intersect line  $t$  at points  $C_1$  making with  $PC_1$  the angle  $\omega$ , the lines  $\{LB_1, PC_1\}$  are parallel. Using this and measuring the angles at  $A_0$ , we find that  $\widehat{A_0PL} = 2\omega - \pi/2$ . On the other side, the center  $K$  of the circle  $\kappa_4$  is on the medial line of  $PA_1$  and since  $\kappa_4$  is tangent to  $B_1A_1$  at  $A_1$ , the line  $A_1K$  passes through  $A_0$ . From the aforementioned tangency follows also that the angle  $\widehat{A_0KT} = \omega$ , point  $T$  being the center of  $\kappa_1$ . Thus, the center  $K$  of  $\kappa_4$  is viewing the fixed segment  $A_0T$  under the fixed angle  $\omega$ . This implies that, as  $A_1$  changes its position on  $\kappa_1$ , the center  $K$ , of the corresponding circle, moves on a circle  $\kappa_0$  passing through the points  $\{A_0, T, P\}$ . Thus, all circles  $\kappa_4$  represent one of the standard ways to generate a cardioid, by fixing a point  $P$  on a circle  $\kappa_0$  and for every other point  $K$  on  $\kappa_0$  drawing the circle  $\kappa_4(K, |KP|)$  ([11, p.35]). The cardioid is then the envelope of all these circles  $\{\kappa_4\}$ . It is also well known that the line, which is simultaneously tangent to the cardioid and the generating it circle  $\kappa_4$ , is the symmetric of the tangent of the circle  $\kappa_4$  at  $P$  w.r. to the tangent of the circle  $\kappa_0$  at the center  $K$  of  $\kappa_4$ . Later applied to  $\kappa_1$ , which represents a special position of  $\kappa_4$ , shows that the line  $t$  is also tangent to the cardioid. Concerning the location of the center  $S$  of the circle  $\kappa_0$ , we notice that the angle  $\widehat{A_0SP} = 2\pi - 4\omega$ , which implies that  $\widehat{SPA_0} = 2\omega - \pi/2 = \widehat{A_0PL}$ .

A short calculation shows also that the radius of  $\kappa_0$  is

$$|PS| = \frac{|PB_1|}{(2 \sin(\omega))^2} = \frac{|PD|}{4 \sin(\omega)^4}.$$

From this follows immediately that

$$|PS| < |PD| \quad \text{precisely when} \quad \omega > \pi/4. \quad (1)$$

On the other side, the cardioid is intimately related to the parabola, since, as is well

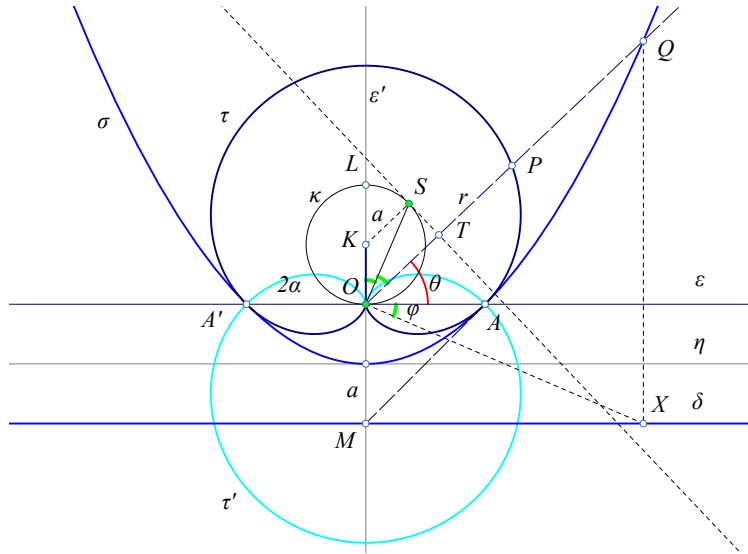


Figure 15. The associated cardioid  $\tau$  of the parabola  $\sigma$

known, the cardioid is the inverse of a parabola, the center of inversion taken at the focus of the parabola ([16, p.91,p.131]). Figure 15 shows the result of inversion of the parabola with equation  $x^2 = 4ay$ , relative to the axis  $\{\eta, \varepsilon'\}$ , consisting of the tangent at the vertex and the axis of the parabola. The inversion is done w.r. to the focus  $O$  and the circle with diameter the *latus rectum*  $AA'$  of the parabola and produces the cardioid  $\tau'$ . Of interest for our discussion is the reflection  $\tau$  of  $\tau'$  w.r. to the latus-rectum line  $\varepsilon$ . This cardioid  $\tau$  is tangent to the parabola at  $\{A, A'\}$ . It is also generated as the envelope of the circles  $\{\kappa_4(S, |SO|)\}$ , for the points  $S$  of the circle  $\kappa(K, a)$ , where  $K$  is the symmetric of the vertex of the parabola w.r. to its focus  $O$ . All these facts are consequences of straightforward calculations, which I leave as an exercise. I call  $\tau$  the “associated to the parabola cardioid”. A short calculation w.r. to the system with axes  $\{\varepsilon, \varepsilon'\}$  shows also that corresponding points  $\{P, Q\}$  on  $\{\tau, \sigma\}$  with the same polar angle  $\theta$  are represented by

$$r = OP = 2a(1 + \sin(\theta)), \quad r' = OQ = \frac{2a}{1 - \sin(\theta)} \quad \Rightarrow \quad r' - r = \frac{2a \sin(\theta)^2}{1 - \sin(\theta)}. \quad (2)$$

This shows that the cardioid  $\tau$  is completely inside the inner domain of the parabola, containing the focus, touching the parabola only at the points  $\{A, A'\}$ .

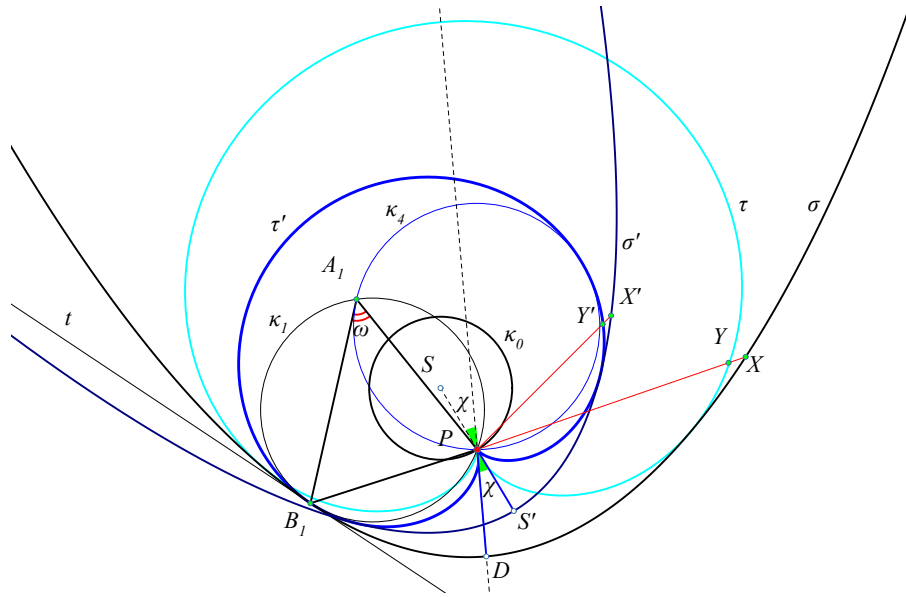


Figure 16. The two parabolas and their associated cardioids

Figure 16 combines the results of the preceding discussion and illustrates the arguments for the proof of the next theorem. The cardioid generated by the circles  $\{\kappa_4\}$  is now denoted by  $\tau'$ , whereas  $\tau$  denotes the associated cardioid of the parabola  $\sigma$ . The two cardioids are connected with a similarity  $f$  with center  $P$ , mapping  $\tau$  onto  $\tau'$ . Point  $P$  and the symmetric  $S'$  of the center  $S$  of the circle  $\kappa_0$  w.r. to  $P$  are respectively the focus and the vertex of a parabola  $\sigma'$ , whose associated cardioid is  $\tau'$ . The similarity  $f$  has its center at  $P$ , its angle is  $\chi = \widehat{DPS'}$  and its ratio is  $k = PS'/PD$ . It is easily seen, that this similarity maps the parabola  $\sigma$  onto  $\sigma'$  and  $\tau$  onto  $\tau'$ .

With this preparation, we can now prove that the cardioid  $\tau'$  has no other than  $B_1$  intersection point with the parabola  $\sigma$ . In fact, assume that  $X$  is a point common to  $\sigma$  and  $\tau'$ . Consider then the point  $Y$  on the position radius  $PX$ , lying on  $\tau$ . From equation 2 we know that  $Y$  is between the points  $\{P, X\}$ . Consider now points  $\{X' = f(X), Y' = f(Y)\}$ . The order relation is preserved by  $f$ . Thus,  $Y'$  is again between the points  $\{P, X'\}$ . But since  $X$  is an intersection point  $X \in \sigma \cap \tau'$ , its image  $X' = f(X)$  must be a point lying between  $\{P, Y'\}$ , which is not possible if  $X \neq B_1$ . Thus, we have proved that if  $\omega > \pi/4$ , then there is no other than  $B_1$  point of intersection of the cardioid  $\tau'$  with the parabola  $\sigma$ . An analogous argument for  $\omega < \pi/4$  shows that there is indeed such an intersection of the corresponding  $\tau'$  with  $\sigma$ . Finally for  $\omega = \pi/4$ , the cardioid  $\tau'$  coincides with the associated cardioid of  $\sigma$  and for this Brocard angle the corresponding self-pivoting quadrangle is easily seen to be a square. Summarizing the previous arguments, we arrive at the proof of the following theorem.

**Theorem 5.** *The Brocard angle of a self-pivoting convex quadrangle of the type  $q(A)^+$  or  $q(B)^+$  is less or equal to  $\pi/4$ , the equality being valid only for the square.*

**6. Types  $q(A)^+$  and  $q(B)^+$  with three equal angles**

Here we continue the analysis of figure 12, of a self-pivoting quadrangle of type  $q(B)^+$ , taking into account general properties of parabolas ([2, p.21], [4, p.28], [17, p.133]), and noticing that the triangles  $\{B_1C_1P, PC_1S_1\}$  are similar. Thus, in the case the circle  $\kappa_4$  and the parabola  $\sigma$  are tangent, then all four points  $\{S_i, T_j\}$  coincide, the three triangles  $\{B_1PC_1, C_1PD_1, D_1PA_1\}$  are similar and three of the angles of the quadrangle are equal. The proof of the following theorem, formulated for the type  $q(B)^+$ , gives a recipe to construct such self-pivoting quadrangles with three equal angles. The analogous theorem for  $q(A)^+$  is also valid. The necessary formulation, as well as minor adaptations and changes for its proof, are left as an exercise.

**Theorem 6.** *The case, of a self-pivoting quadrangle of type  $q(B)^+$ , in which the circle  $\kappa_4$  is tangent to the parabola  $\sigma$  and the triangles  $\{B_1PC_1, C_1PD_1, D_1PA_1\}$  are similar, is, up to similarity, completely determined by the angle  $\phi$  of the triangles at the pivot point  $P$ .*

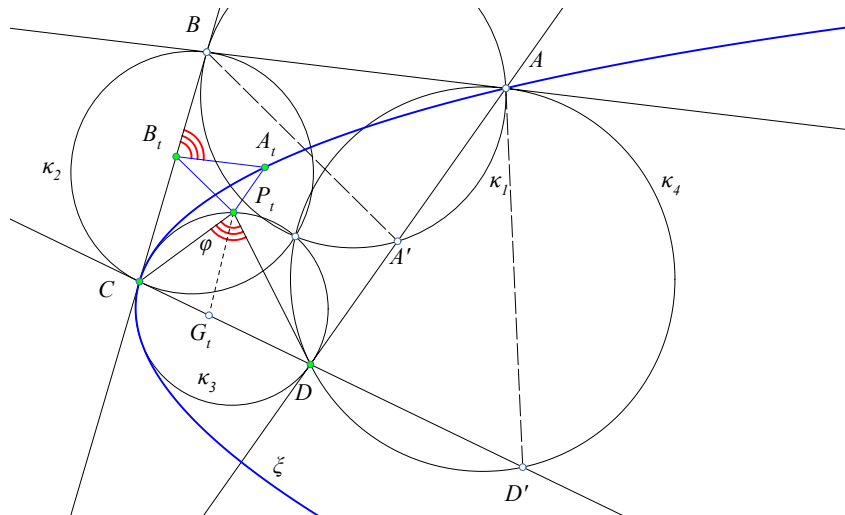


Figure 17. Self-pivoting quadrangle of type  $q(B)^+$  with three equal angles

*Proof.* Figure 17 shows the recipe to construct such a self-pivoting quadrangle of type  $q(B)^+$ , up to similarity and from a given angle  $\phi$  at  $P$ . The construction starts with a circle  $\kappa_3$  and a chord of it  $CD$ , viewed from points of the circle under the angle  $\phi$  or its supplement. Taking such a point  $P_t \in \kappa_3$ , we define the similarity transformation  $f_t$  ([3, ch.IV]) with center at  $P_t$ , rotation angle  $\phi$  and similarity ratio  $k_t = P_tC/P_tD$ . The image  $B_t = f_t(C)$  of  $C$  under the

similarity defines the triangle  $P_t B_t C \sim P_t C D$  and applying  $f_t$  once more we obtain  $A_t = f_t(B_t) = f_t^2(C)$  and the triangle  $P_t A_t B_t \sim P_t B_t C$ . As  $P_t$  varies on the circle  $\kappa_3$ , the corresponding point  $A_t = f_t^2(C)$  moves on a parabola  $\xi$ . This is an immediate consequence of two facts. The first, following from a simple angle chasing argument, is that the line  $A_t B_t$  makes the angle  $\phi$  with the tangent  $CB$  of  $\kappa_3$  at  $C$ . The second fact, following directly from the definitions, is that the ratio  $A_t B_t / B_t C = k_t$ .

Combining these two facts, we can find a simple parametrization of the variable point  $A_t$ , showing that it moves on a parabola. For this we use the bisector  $P_t G_t$  of the angle  $\phi$  at  $P_t$ , which divides the side  $CD$  at the ratio  $k_t = t / (a - t)$ , where  $a = CD$ . Then setting  $x = CB_t$  and  $y = B_t A_t$ , we see that

$$\frac{x}{a} = k_t = \frac{t}{a-t}, \quad \frac{y}{x} = k_t \Rightarrow x = a \frac{t}{a-t}, \quad y = a \frac{t^2}{(a-t)^2},$$

which is a parametrization of a parabola in oblique axes. The point  $A$  is an intersection of the parabola with the tangent  $DA$  of  $\kappa_3$  at  $D$  and point  $B$  is the intersection of  $CB$  with the parallel to  $A_t B_t$ , making with  $BC$  the angle  $\phi$ . From its definition follows that the quadrangle  $ABCD$  is self-pivoting of type  $q(B)^+$  with pivot  $P$ , coinciding with the second intersection of the circles  $\{\kappa_3, \kappa_2\}$ , where  $\kappa_2$  is the circle tangent to  $CD$  at  $C$ , passing through  $B$ .  $\square$

It is easy to see that if  $\phi = \pi/2$ , then the quadrangle  $ABCD$  is a square. In general, since the three angles of the quadrangle are equal to  $\pi - \phi$ , the magnitude of the angle is restricted by the inequalities for the fourth angle at  $D$

$$\widehat{D} = 2\pi - 3(\pi - \phi) = 3\phi - \pi \quad \text{and} \quad 0 < \widehat{D} < \pi \quad \Rightarrow \quad 60^\circ < \phi < 120^\circ.$$

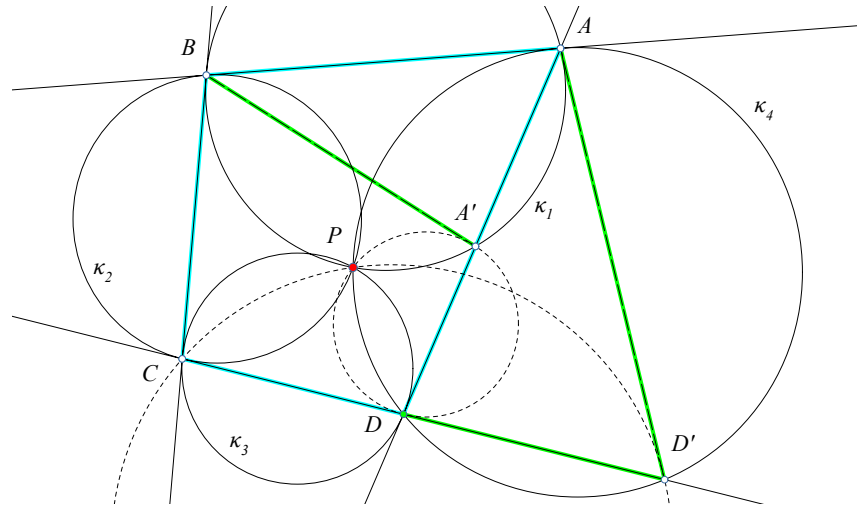


Figure 18. The similar quadrangles  $ABCD \sim BCDA' \sim D'ABC$

Figure 18 shows another characteristic of this class of quadrangles, determined, up to similarity from an angle  $\phi$  satisfying the above restriction. The other in-



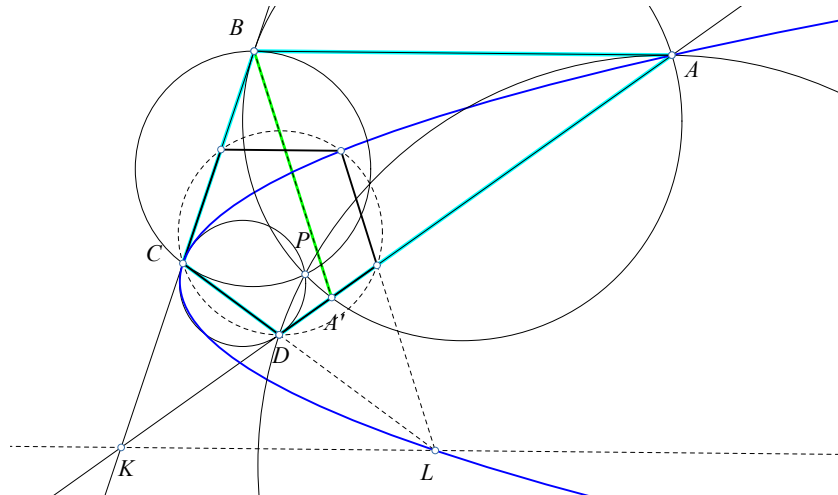


Figure 19. Self-pivoting quadrangle from a regular pentagon

tersection points  $\{A', D'\}$  of the two circles  $\{\kappa_1, \kappa_4\}$  correspondingly with sides  $\{AD, DC\}$  define similar quadrangles  $ABCD \sim BCDA' \sim D'ABC$ . It is also easily verified that the new quadrangles are self-pivoting about the same point  $P$  with the original one. Figure 19 shows one more example of a self-pivoting quadrangle of the type  $q(B)^+$ . It is the one with three angles equal to  $108^\circ$ , the angle of the regular pentagon. By the previous restriction for the angles and the discussion so far, follows that the rectangle and the pentagon are the only regular polygons, whose angles may appear in this kind of self-pivoting quadrangles. Notice that in this case the axis of the parabola  $\xi$  is parallel to the line  $KL$ , which is parallel to a diagonal of the pentagon.

### 7. Self-pivoting quadrangles of types $q(C)^+$ and $q(D)^+$

As noticed in section 3, these two types of self-pivoting quadrangles have similar arrangements of vertices, leading to identical geometric properties. For this reason we confine our discussion to one of them, the type  $q(C)^+$ , and make some remarks on the differences for the related type  $q(D)^+$ , at the end of the section. In the type  $q(C)^+$  the circumscribing  $q$ , which is similar to the circumscribed  $q_1$ , has opposite to  $A_1B_1$  the angle  $\widehat{C}$  and the orientation of the two quadrangles is the same. Next theorem shows that the requirement of self-pivoting of this type is quite restrictive for the quadrangle.

**Theorem 7.** *A convex self-pivoting quadrangle of the type  $q(C)^+$  is necessarily a trapezium of a special kind, for which the circles  $\{\kappa_2, \kappa_4\}$  are equal. The trapezium in this case defines another isosceles trapezium inscribed in  $\kappa_2$  called the “core” of  $q$ . Each isosceles trapezium is the core of two, in general, different trapezia, which are self-pivoting of type  $q(C)^+$ .*

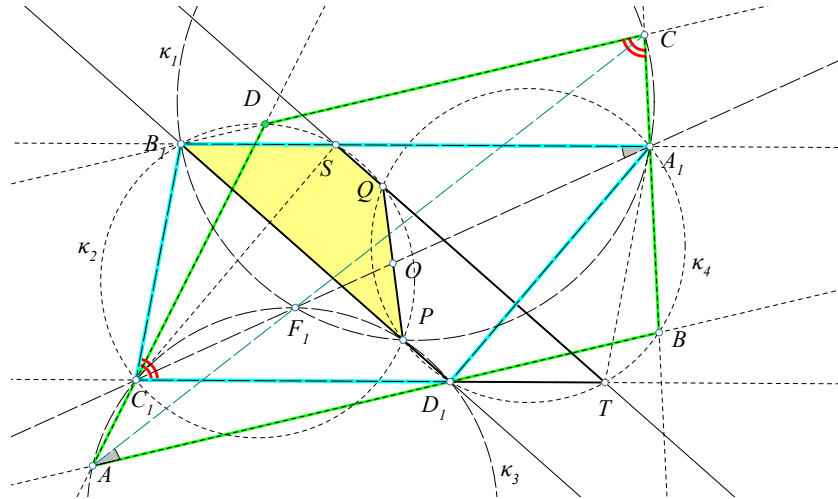


Figure 20. Self-pivoting quadrangle of the type  $q(C)^+$  is a trapezium

*Proof.* Figure 20 shows a quadrangle of this type together with the corresponding isosceles trapezium  $\tau = QSB_1P$ , which is the *core* of the quadrangle  $q_1$ . In order to define it, start with  $q_1$  and consider the second intersection points  $\{S, T\}$  of  $\{\kappa_2, \kappa_4\}$  respectively with  $\{A_1B_1, C_1D_1\}$ . A simple angle chasing shows that lines  $\{C_1S, A_1T\}$  are respectively tangent to the circles  $\{\kappa_3, \kappa_1\}$ . For  $A_1T$  this follows from the equality of angles

$$\widehat{CB_1A_1} = \widehat{CF_1A_1} = \widehat{C_1F_1A} = \widehat{C_1D_1A} = \widehat{BD_1T} = \widehat{BA_1T}.$$

Analogously is seen the other tangency. This implies that  $C_1TA_1S \sim ABCD$  is a position of the pivoting quadrangle  $ABCD$ . The similarity of the triangles  $A_1B_1C_1 \sim ABC$  implies then that  $\widehat{B_1A_1C_1} = \widehat{A_1C_1T}$ , which shows that the lines  $\{A_1B_1, C_1D_1\}$  are parallel. From this follows immediately that  $SC_1D_1A_1, B_1C_1TA_1$  are parallelograms and  $\{SB_1C_1, D_1TA_1\}$  are equal triangles. This implies in turn that the circles  $\{\kappa_2, \kappa_4\}$  are equal, since the equal segments  $\{C_1S, D_1A_1\}$  are respectively seen from  $\{B, T\}$  under equal angles.

Combining these facts, we see that the whole figure can be reproduced from the two glued, equal to the core, isosceles trapezia  $\{B_1SQP, QPD_1T\}$ . In fact, if we start from these two equal trapezia and their circumcircles  $\{\kappa_2, \kappa_4\}$ , then the missing vertices  $\{A_1, C_1\}$  can be defined as intersections of these circles respectively with the lines  $\{BS, D_1T\}$ . Figure 21 shows how the self-pivoting trapezium is defined from the isosceles trapezium  $B_1SQP$ . In fact, starting with the arbitrary isosceles trapezium  $B_1SQP$  we define its symmetric  $QPD_1T$  w.r to the middle  $O$  of the non parallel side  $PQ$ . The missing vertices lie on respective circumcircles of the trapezia and are symmetric w.r to  $O$ . Thus, there result two acceptable solutions  $\{A_1B_1C_1D_1, A'_1B_1C'_1D_1\}$  i.e. self-pivoting quadrangles of the type  $q(C)^+$  about the point  $P$ .  $\square$

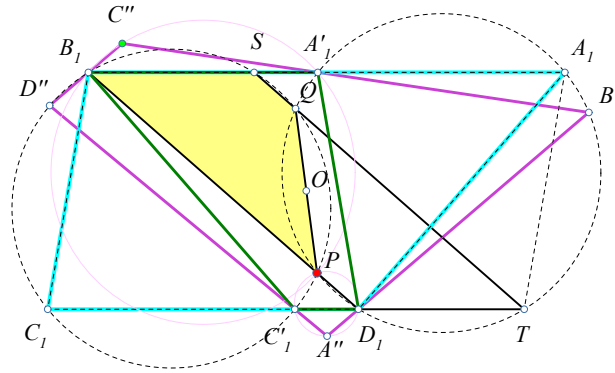


Figure 21. The two cases defined by the trapezium  $ABCD$

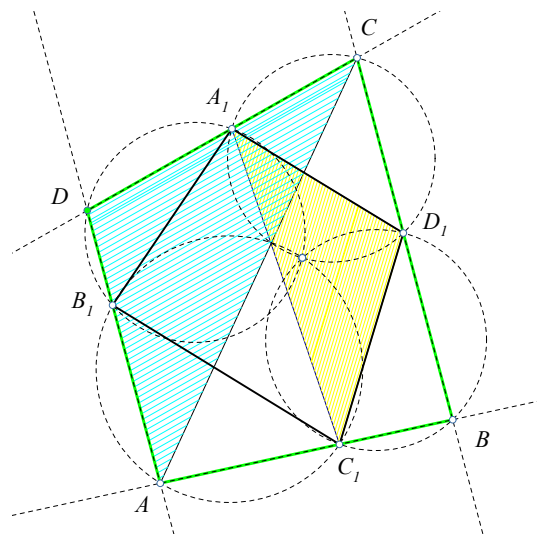


Figure 22. Self pivoting quadrangle of the type  $q(D)^+$

The arguments used in the discussion of the type  $q(C)^+$  apply almost verbatim to the case of  $q(D)^+$  and lead to a similar result. The quadrangle is again a trapezium of the kind, referred to in the previous theorem.

**Theorem 8.** *A convex self-pivoting quadrangle of the type  $q(D)^+$  is necessarily a trapezium of the special kind, considered in theorem 7.*

Figure 22 shows a characteristic case of a self-pivoting of type  $q(D)^+$ . The only difference is in the arrangement of parallel sides. Here the parallel sides are  $\{A_1D_1, B_1C_1\}$ , whereas in the previous case the parallels are  $\{A_1B_1, C_1D_1\}$ .

**Corollary 9.** *The only self-pivoting convex quadrangle w.r. to all types of positive pivoting is the square.*

*Proof.* By *positive pivoting* we mean the types  $\{q(A)^+, q(B)^+, q(C)^+, q(D)^+\}$ . If the quadrangle  $q_1$  is of the first two types simultaneously, then, by theorem 2 it is harmonic. If it is also simultaneously of the two last types, then, by the theorems of this section, it is also a parallelogram. But the only harmonic parallelogram is the square.  $\square$

**8. Self-pivoting of types  $\{q(A)^-, q(B)^-, q(C)^-, q(D)^-\}$**

These four types of self-pivoting quadrangles, have some common traits, noticed in section 3. They are precisely the types that have exactly two opposite vertices with the ASV property. The main consequence of this is given by the next theorem.

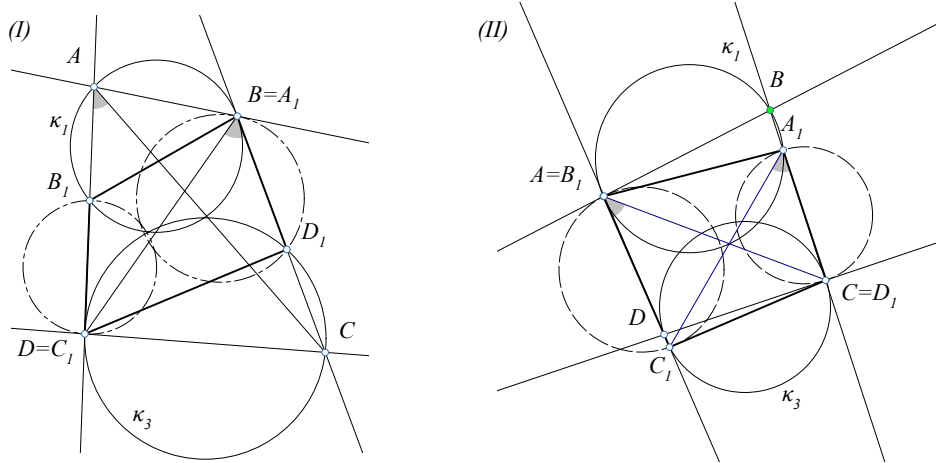


Figure 23.  $\{q(A)^-, q(B)^-\}$  have two opposite vertices with the ASV property

**Theorem 10.** *The self-pivoting quadrangles of the types  $q(A)^-, q(B)^-, q(C)^-, q(D)^-$  are cyclic.*

*Proof.* The proof relies on the fact, that the vertices of the circumscribing pivoting quadrangle  $q = ABCD$  with the ASV property move on circles which are tangent to two opposite sides of the circumscribed quadrangle  $q_1 = A_1B_1C_1D_1$  (See Figure 23). Working with the type  $q(A)^-$ , we notice that there is a position of the circumscribing  $q$ , for which we have identification of two opposite vertices with corresponding two vertices of the circumscribed  $q_1$ . The vertices are  $B = A_1$  and  $D = C_1$  (See Figure 23-I). Consequently also the side-lines  $\{A_1D_1 = BC, B_1C_1 = AD\}$ . This is valid also in the case of type  $q(B)^-$  (See Figure 23-II), and also in the remaining two types. This identification of vertices and side-lines is, more generally, valid also in the case the two quadrangles  $\{q, q_1\}$  have the same angles and the correct arrangement of the angles, according to the circumscription type under consideration, even if they are not similar, as is the case with the two configurations for  $q(A)^-$  and  $q(B)^-$  in figure 23. If however the quadrangles  $\{q, q_1\}$  are similar, then the side  $CD$  resp.  $C_1D_1$  is viewed from the vertices  $\{A, A_1 = B\}$  resp.  $\{A_1, A = B_1\}$  under the same angle. This proves

that the quadrangles are cyclic for the two types  $\{q(A)^-, q(B)^-\}$ , the proof for the remaining two types being exactly the same.  $\square$

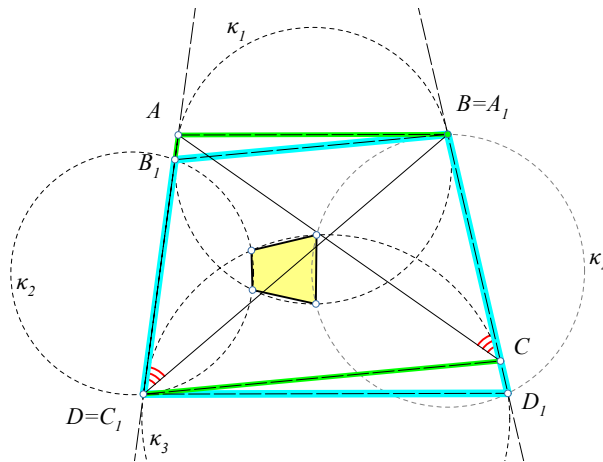


Figure 24. Trying to draw a quadrangle of type  $q(A)^-$

Figure 24 shows how to draw a cyclic quadrangle  $q_1$  and a particular circumscribing  $q$  of the type  $q(A)^-$  allowing a quick construction of the circles  $\{\kappa_i\}$ . The condition on the angles implies that  $(A_1B_1, CD)$  and  $(AB, C_1D_1)$  are pairs of parallels. It is also easily seen, that drawing in an arbitrary cyclic quadrangle  $q_1$  parallels  $\{A_1A, C_1C\}$  to opposite sides we obtain a new cyclic quadrangle  $q = ABCD$ , with the same angles as  $q_1$ . Figure 24 shows such a general construction from an arbitrary cyclic quadrangle  $q_1$ . In order to obtain a self-pivoting one we must succeed to have four points coincident. These are the second intersections of adjacent circle pairs  $\{\kappa_1 \cap \kappa_2, \kappa_2 \cap \kappa_3, \dots\}$ , their quadrangle shown also in the figure. Next theorem shows how this is done. The proof again is given in detail only for the type  $q(A)^-$ , the other cases allowing a completely analogous handling.

**Theorem 11.** *The self-pivoting quadrangles of type  $q(A)^-, q(B)^-, q(C)^-, q(D)^-$  are necessarily cyclic quadrangles. Given a cyclic quadrangle  $q_0$ , there is, up to similarity, precisely one self-pivoting quadrangle  $q_1$  of each of these types, with the same angles and the same succession of angles as  $q_0$ .*

*Proof.* The first part of the theorem follows from the preceding discussion. To show the second part for the type  $q(A)^-$ , we consider the arbitrary fixed convex cyclic quadrangle  $q_0 = A_0B_0C_0D_0$  and the family of other cyclic quadrangles  $q' = ABC_0D_0$ , produced by varying one of its sides  $(AB)$  parallel to itself (See Figure 25). In order to locate the self-pivoting among all these quadrangles we exploit the fact that, for this type of self-pivoting, the circles  $\{\kappa_1, \kappa_3, \kappa_4\}$  are respectively tangent to  $\{A_0D_0, B_0C_0, AB'\}$  at the points  $\{A, C_0, A\}$ , where  $AB'$  is parallel to  $C_0D_0$ . In this case the self-pivoting quadrangle results when, for varying  $A$  on  $\varepsilon = A_0D_0$ , the second intersection point  $P$  of the circles  $\{\kappa_1, \kappa_4\}$  takes a

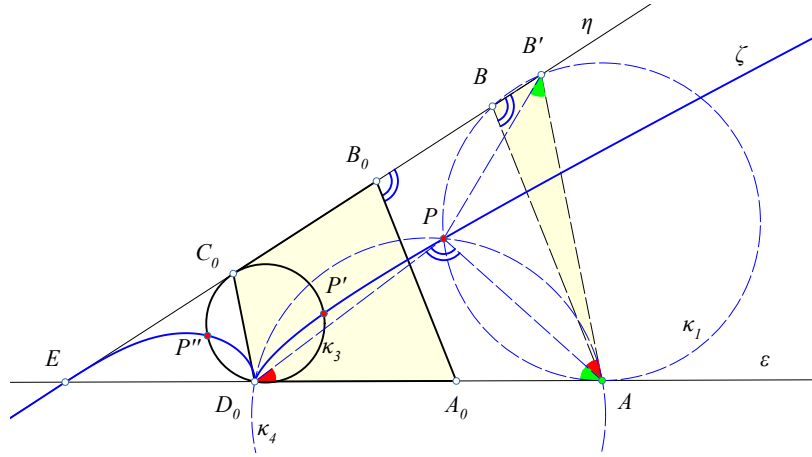


Figure 25. Seeking a self-pivoting quadrangle of type  $q(A)^-$  with given angles

position on the circle  $\kappa_3$ . But as the point  $A$  varies on  $\varepsilon$ , the lemmata below show that the corresponding point  $P$  describes a cubic curve  $\zeta$  having a singular point at  $D_0$  and intersecting the circle  $\kappa_3$  at two other points  $\{P', P''\}$ , leading to two similar quadrangles with the desired properties. The determination of the whole quadrangle from the point  $P$  is trivial, since the angle

$$\delta = \widehat{A_0D_0C_0} = \widehat{D_0PA} = \widehat{APB'},$$

remains constant for all positions of  $P$ . Hence, having the position of  $P$ , we can draw the angle  $\widehat{D_0PA} = \delta$  and find the position of  $A$ , from which the parallel to  $A_0B_0$  determines the whole quadrangle.

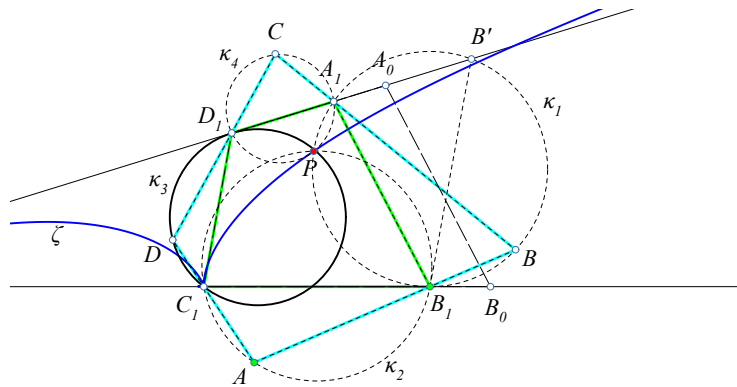


Figure 26. The cubic determining the self-pivoting  $q_1 = A_1B_1C_1D_1$  of type  $q(B)^-$

The proof for the other types is the same. Figure 26 shows e.g. the corresponding cubic for the type  $q(B)^-$ . In this case the cubic is the geometric locus of the second intersection points  $\{P\}$  of the circles  $\{\kappa_1, \kappa_2\}$ , circle  $\kappa_1$  being tangent to

$B_1C_1$  at  $B_1$  and passing through  $A_1$ , as  $B_1$  moves on line  $C_1B_0$ . The circle  $\kappa_2$  is tangent to the parallel  $B_1B'$  to  $C_1D_1$  and passes through  $C_1$ . Here we start again from an arbitrary cyclic quadrilateral  $A_0B_0C_1D_1$  and draw parallels  $A_1B_1$  to  $A_0B_0$  seeking the position of  $B_1$ , which defines the self-pivoting quadrangle  $q_1$ . The figure shows the appropriate position of the pivot  $P$ , which is the intersection of the cubic with  $\kappa_3$ . It shows also a pivoting quadrangle  $q = ABCD \sim q_1$  circumscribing  $q$ .  $\square$

In the rest of this section we discuss in detail the case of the cubic  $\zeta$  related to the type  $q(A)^-$ , the arguments for the cases  $\{q(B)^+, \dots\}$  and the cubics related to these types being completely analogous.

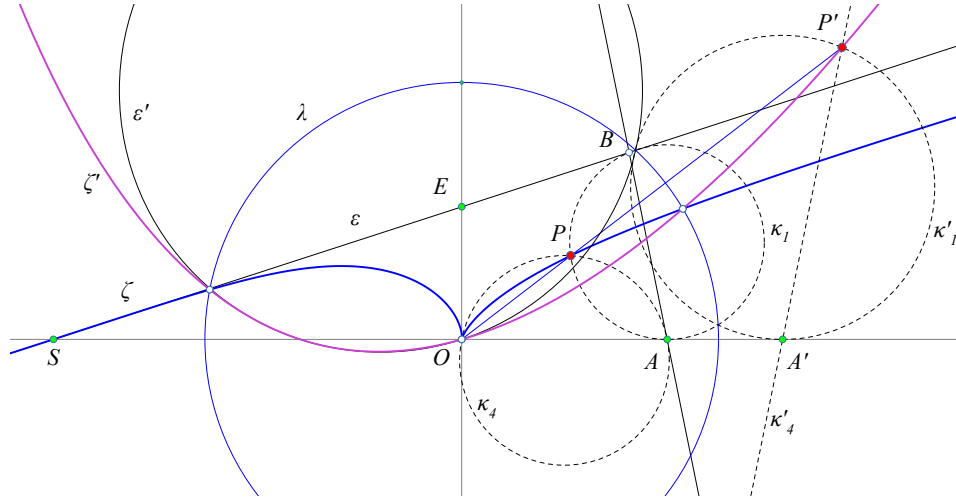


Figure 27. The cubic carrying the points  $P$

**Lemma 12.** *Under the notation and conventions of theorem 11, for the type  $q(A)^-$ , the intersection point  $P$  of the circles  $\{\kappa_1, \kappa_4\}$  describes a cubic curve.*

*Proof.* Referring to figure 25, we use cartesian coordinates with origin  $O$  at the vertex  $D_0$  of the quadrangle  $q_0$  and identify the  $x$ -axis with the line  $D_0A_0$ . The line  $AB$  moves parallel to itself with  $A$  on the  $x$ -axis. Also  $B$  is on the fixed line  $\varepsilon = A_0B_0$ . The point  $P$  is on the circle  $\kappa_1$ , which is tangent to the  $x$ -axis at  $A$  and passes through  $B$ . It is also on the circle  $\kappa_4$ , which is tangent to  $AB$  at  $A$  and passes through the origin  $O$ . Now we consider the inversion  $f$  w.r. to a fixed circle  $\lambda$  centered at  $O$  (See Figure 27). By this the image  $\varepsilon' = f(\varepsilon)$  is a fixed circle,  $\kappa'_1 = f(\kappa_1)$  is a circle tangent to the  $x$ -axis and intersecting the circle  $\varepsilon'$  under a fixed angle, and  $\kappa'_4 = f(\kappa_4)$  is a line passing through  $A' = f(A)$  and having a fixed direction. Thus the inverted  $P' = f(P)$  is the intersection of a line  $\kappa'_4$  and a circle  $\kappa'_1$  passing through  $A'$  tangent there to the  $x$ -axis and cutting the fixed circle  $\varepsilon'$  under a fixed angle. Next lemma shows that the geometric locus  $\zeta'$  of such points  $P'$  is a parabola passing through the origin and having the form

$$(px + qy)^2 - rx - sy = 0.$$

This, taking again the inverted in the form  $(x, y) = f(x', y') = k(x', y')/(x'^2 + y'^2)$ , with a constant  $k$ , shows that the inverted of the parabola  $\zeta = f(\zeta')$  satisfies the cubic equation

$$k(px + qy)^2 - (rx + sy)(x^2 + y^2) = 0.$$

□

**Lemma 13.** *A point  $A$  moves on the fixed line  $\varepsilon$ , and the line  $\eta$  through  $A$  has a fixed direction. The circle  $\kappa(X, r)$  is tangent to  $\varepsilon$  at  $A$  and intersects a fixed circle  $\lambda(K, r_0)$  passing through  $O \in \varepsilon$  under a fixed angle  $\phi$ . Then, the geometric locus*

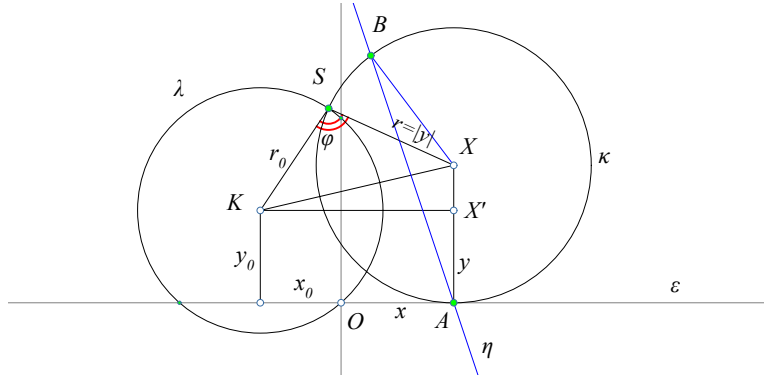


Figure 28. The parabola of points  $B$

of the second intersection point  $B$  of  $\eta$  and  $\kappa$  is a parabola through the point  $O$ .

*Proof.* Using the point  $O$  as origin and the line  $\varepsilon$  as  $x$ -axis of a cartesian coordinate system, in which  $K = (x_0, y_0)$ , we find that the center  $X$  of the variable circle  $\kappa$  satisfies the parabola equation (See Figure 28)

$$x^2 - 2x_0x - 2(y_0 - r_0 \cos(\phi))y = 0.$$

On the other side the intersection point  $B(x', y')$  of  $\kappa$  and the line  $\eta$  in fixed direction can be expressed in terms of  $X(x, y)$  and a fixed unit vector  $e = (e_1, e_2)$  by the equations

$$B = X + ye \quad \Leftrightarrow \quad x' = x + ye_1, \quad y' = y + ye_2.$$

This means that  $B$  describes the affine transformation of a parabola, which is also a parabola with the desired properties. □

**Lemma 14.** *Under the notation and conventions of this section, the two quadrangles, created from the intersection points  $\{P', P''\}$  of the cubic  $\zeta$ , of theorem 11 for the type  $q(A)^-$ , with the circle  $\kappa_3$ , are similar and inversely oriented. The points  $\{P', P''\}$  are isogonal conjugate w.r. to the angle  $\widehat{C_1ED_1}$ .*



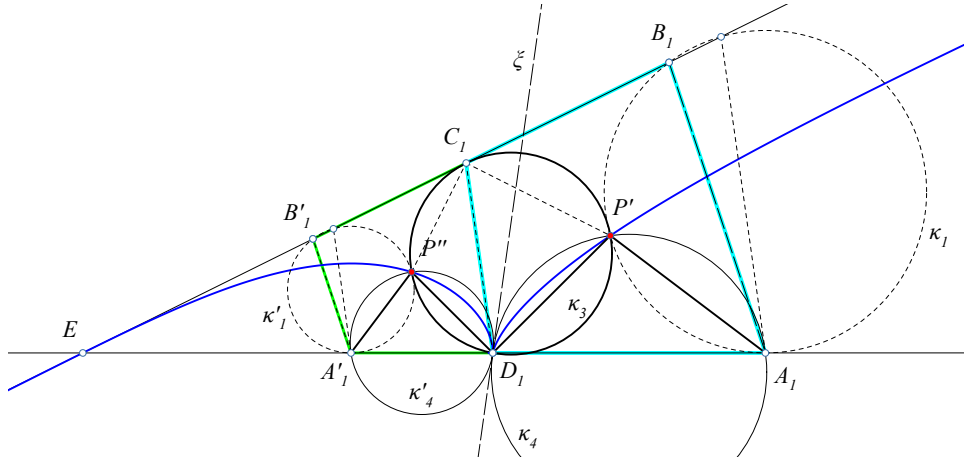


Figure 29. The two similar quadrangles of type  $q(A)^-$

*Proof.* The fact that there are precisely two such intersection points follows from the geometric definition of the points  $P$  of the cubic  $\zeta$ . The cubic has a singular point at  $D_1$  and its limit tangents at  $D_1$  from the two branches coincide with the line  $\xi$ , which is symmetric to  $D_1C_1$  w.r. to  $D_1A_1$  (See Figure 29). The circles  $\{\kappa_4, \kappa'_4, \dots\}$  for the various positions of  $P$  are members of the pencil of circles tangent to  $\xi$  at  $D_1$ . This implies geometrically that there are two intersection points of the cubic with  $\kappa_3$  lying on either sides of  $\xi$ . It is also easily seen geometrically that the two resulting solutions are similar and inversely oriented. That there are no more intersection points follows from the fact that the cubic and the circle  $\kappa_3$  are inverses under  $f$  respectively of a parabola and a line, which can have no more than two intersection points.  $\square$

### 9. Self-pivoting quadrangles of type $q(C)^-$

In the previous section we saw that a self-pivoting quadrangle, whose type coincides with one of  $\{q(A)^-, q(B)^-, q(C)^-, q(D)^-\}$ , is necessarily cyclic. We saw further that, given a convex cyclic quadrangle  $q_0$ , there is, up to similarity, precisely one self-pivoting quadrangle  $q_1$  of each one of these types, with the same angles and the same succession of angles as  $q_0$ . Next theorem shows that this  $q_1$ , in the case of the type  $q(C)^-$ , satisfies a stronger condition.

**Theorem 15.** *The only self-pivoting quadrangles of type  $q(C)^-$  are the harmonic quadrangles.*

*Proof.* Constructing the self-pivoting of this type by the method of the previous section, we start with an arbitrary cyclic quadrangle  $q_0 = A_0B_1C_1D_0$ , with fixed given angles, and an arbitrary point  $D_1$  moving on the line  $C_1D_0$ . From  $D_1$  we draw the parallel  $D_1A_1$  to  $D_0A_0$  and consider the variable circles  $\kappa_3$  tangent to  $D_1A_1$  at  $D_1$  and passing through  $C_1$  and  $\kappa_4$  tangent to  $C_1D_1$  at  $D_1$  and passing through  $A_1$ . Their intersection point  $P$  describes, as  $D_1$  moves on  $C_1D_0$ , a cubic  $\zeta$ .

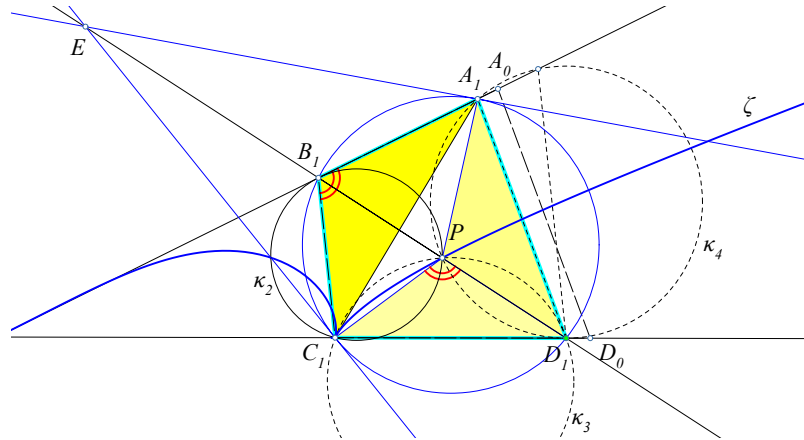


Figure 30. Constructing a quadrangle of type  $q(C)^-$

This is exactly the same situation as in the preceding section. The difference from that is now that the similar triangles  $\{PC_1D_1, PD_1A_1\}$  have their angle at  $P$  equal to  $\widehat{B_1}$ , while in the previous case this angle was equal to  $\widehat{C_1}$ . The equality of the angles implies now that the intersection point  $P$  of the cubic with the fixed circle  $\kappa_2$ , which is tangent to  $B_1A_1$  at  $B_1$  and passes through  $C_1$ , is on the diagonal  $B_1D_1$ . This follows trivially from the equality of the angles  $\widehat{B_1PC_1} = \pi - \widehat{C_1B_1A_1}$ . Then, an equally simple angle chasing argument shows that the two similar triangles  $\{PC_1D_1, PD_1A_1\}$  are also similar to the triangle  $A_1B_1C_1$ , which is a characteristic property of the harmonic quadrangles ([12]).  $\square$

There are several partial results that could be produced as corollaries of the previous discussion. Corollaries concerning self-pivoting of quadrangles w.r. to combinations of some types, or/and corollaries concerning such combinations and some particular kinds of quadrangles, like rectangles, parallelograms, trapezia etc, all left as exercises for the interested reader.

## References

- [1] A. Akopyan, Geometry of the cardioid, *Amer. Math. Monthly*, 121 (2013) 1–6.
- [2] A. Akopyan and A. Zaslavsky, *Geometry of Conics*, American Mathematical Society, New York, 2012.
- [3] W. Barker and R. Howe, *Continuous Symmetry, From Euclid to Klein*, American Mathematical Society, 2007.
- [4] W. H. Besant, *Elementary Conics*, George Bell and Sons, London, 1901.
- [5] J. Booth, *A treatise on some new geometrical methods*, I, II, Longmans, London, 1873.
- [6] F. Brown, Brocard points for a quadrilateral, *Math. Gazette*, 9:83?85, 1917.
- [7] W. Gallatly, *The Modern Geometry of the Triangle*, Francis Hodgson, London, 1913.
- [8] R. Johnson, *Advanced Euclidean Geometry*, Dover Publications, New York, 1960.
- [9] T. Lalesco, *La Geometrie du triangle*, Librairie Vuibert, Paris, 1952.
- [10] D. Lawrence, *A Catalog of Special Plane Curves*, Dover Publications, New York, 1972.
- [11] E. Lockwood, *A Book of Curves*, Cambridge university press, Cambridge, 1961.
- [12] P. Pamfilos, The associated harmonic quadrilateral, *Forum Geom.*, 14 (2014) 15–29.

- [13] C. Pohoata, Harmonic quadrilaterals revisited, *Gazeta Matematica*, seria A, 29 (2011) 15–35.
- [14] R. Proctor, *The Geometry of Cycloids*, Longmans, Green and Co., London, 1878.
- [15] G. Salmon, *A treatise on Conic Sections*, Longmans, Green and Co., London, 1917.
- [16] H. Wieleitner, *Spezielle Ebene Kurven*, Goeschensche Verlagshandlung, Leipzig, 1908.
- [17] C. Zwikker, *The Advanced Geometry of Plane Curves and Their Applications*, Dover, New York, 1963.

Paris Pamfilos: University of Crete, Greece  
E-mail address: pamfilos@uoc.gr